Conformation of Spacers in Smectic Poly(ester imide)s

CHRISTOPH WUTZ, DANA SCHLEYER

Institut für Technische und Makromolekulare Chemie, Universität Hamburg, Bundesstrasse 45, D-20146 Hamburg, Germany

Received 23 June 1997; revised 19 February 1998; accepted 3 March 1998

ABSTRACT: Several poly(ester imide)s based on 4-N-(carboxyphenyl)trimellitimide, 4-N-(carboxyethenylphenyl)trimellitimide, 4-hydroxy-N-(4-hydroxyphenyl)phthalimide and long aliphatic spacers have been investigated by different solid-state NMR techniques. The conformations of the methylene units were studied by the γ-gauche effect of the ^{13}C chemical shift. In the frozen smectic LC phase, an alternating sequence of trans-conformations and disordered segments is predominant. In contrast, the spacers in the smectic-crystalline phase are capable of forming ordered trans–trans conformations. The amount of tt-conformations is found to increase with the spacer length and depend on the packing of the mesogens and the type of linkage between mesogen and spacer. The thermal stability above 100°C and the segmental mobility of the tt-conformations, as measured by $^{13}C/^{1}H$ wide line separation NMR, suggest a ropelike arrangement of the spacers. The tt-sequences are located in the outer parts rather than in the center of the spacer layer. Dephasing delay experiments on analogous polymers, which are deuteriated selectively in the four central methylene groups of the spacers, prove that these segments do not contain tt-conformations. Consequently, the ordering is due to the molecular constrains exerted by the rigid mesogenic groups and not by lateral van der Waals interactions between adjacent spacer segments. In a random copolymer with two different spacer lengths, the shorter spacer is found to be more extended than in the corresponding homopolymer. J Polym Sci B: Polym Phys 36: 2033–2046, 1998

Keywords: spacer conformation; solid-state ^{13}C NMR; smectic; poly(ester imide)s

INTRODUCTION

This article is part of a broader study on structure and properties of polymers forming layer structures. One group of such layer polymers consists of a regular sequence of rigid, polar mesogens and flexible, nonpolar spacers in the main chain. These polymers tend to form smectic layer structures either in the liquid-crystalline (LC) phase or in the solid state. Several publications report on the chain-packing and phase behavior of such polymers, but are mostly focussed on orientation and packing of the mesogens.[1–7] Furthermore, this special polymer structure virtually fixes both ends of the spacer and, therefore, reduces the possible conformations. In this respect, the study of such a model system should provide deeper insight into the general behavior of alkane chains. However, publications concerning the conformation or mobility of the spacers are comparatively rare and often refer to polymer systems that exclusively form nematic phases.[8–10] Recently, Cheng et al. reported on the conformation of methylene groups in smectic polyethers.[11]

This article will demonstrate that the incorporation of the mesogens into the smectic layer structure affects the properties of the spacer significantly. Poly(ester imide)s (PEI) of the chemical structures 1, 2, and 3 (Fig. 1) exhibit a particularly high tendency of forming layers due to their large differences in the polarities of mesogens and

Correspondence to: C. Wutz

Journal of Polymer Science: Part B: Polymer Physics, Vol. 36, 2033–2046, (1998)
 CCC 0887-6266/98/122033-14

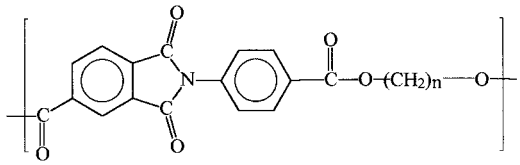

PEI 1 n = 12, 16, 22

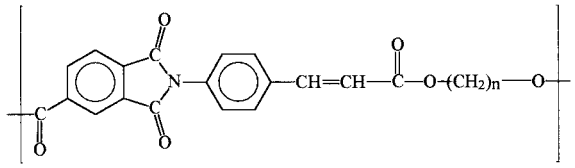

PEI 2 n = 12, 16, 22

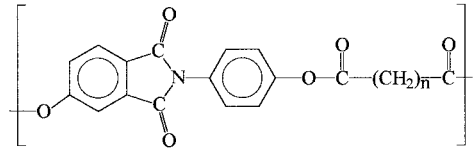

PEI 3 n = 12, 20

Figure 1. Chemical structures of the investigated poly(ester imide)s (PEI) 1, 2, and 3.

spacers. Wide-angle X-ray scattering (WAXS) powder and fiber patterns, polarized light microscopy, and differential scanning calorimetry (DSC), demonstrate that the PEI form various smectic liquid-crystalline (LC) and smectic-crystalline phases, the formation of which depend on the chemical structure of the mesogen, the spacer length, and the thermal treatment.[2,3,12,13] PEI 1 and 3 are isomers with a different orientation of the carboxylate groups and it has been previously demonstrated that the inversion of the carboxylate strongly influences the mesogenic character and, thereby, the phase behavior. In the PEI 2, the mesogen is lengthened in contrast to PEI 1 by the introduction of the ethenyl group, which allows a photochemical crosslinking of the mesogens. However, the present study is focused on the conformation of the spacers between the smectic mesogen layers in the solid state.

For the investigation of the chain conformation, NMR spectroscopy has proved to be a powerful tool. It is widely known from studies of polyethylene[14] and alkane side chains,[15] that the conformation of an alkane chain can be determined by solid-state ^{13}C NMR under the condition of cross-polarization (CP), magic-angle spinning (MAS), and dipolar decoupling (DD) via the γ-gauche effect of the ^{13}C chemical shift.[16] For a methylene group of an alkyl chain, the chemical shift of the carbon under observation is determined by the conformation of its two substituents in the γ position. The gauche conformation exerts more shielding than the trans-conformation, and therefore, the ^{13}C NMR resonances of conformational disordered segments occur at a higher field. For example, the trans–trans conformations of the crystalline regions of polyethylene give rise to a signal at about 34 ppm; while the ^{13}C chemical shift of the amorphous phase is found to range between 30 and 31 ppm, depending on the temperature. However, in a smectic system, the conformation of the spacer segments is influenced by the appendance to the mesogenic groups. Previous investigations demonstrated that the PEI 2 and 3 with long aliphatic spacers can contain *trans–trans* conformations.[12,13]

EXPERIMENTAL

Materials

The poly(ester imide)s were synthesized and characterized by Dr. Nicolas Probst in the group of Dr. H. R. Kricheldorf.[12,13,17] The detailed synthetic procedure and basic properties have been reported in earlier publications. The polymers were dissolved in CH_2Cl_2/trifluoroacetic acid, precipitated into methanol, and subsequently annealed at 140°C for 24 h under vacuum. The quenched samples were melt-pressed at 200°C and quenched rapidly into ice water.

Measurements

The NMR spectra were recorded on a Bruker MSL 300 spectrometer (7.05 Tesla) at a ^1H frequency of 300.13 MHz. ^{13}C solid state NMR, using cross-polarization, magic-angle spinning (CP/MAS), and depolar decoupling, was performed between 20°C and 140°C at 75.47 MHz using a double-bearing variable temperature Bruker MAS probe, 7 mm zirconium oxide rotors, 5000 Hz spinning rate, 1 ms contact time, and 4 s recycle delay. About 1000 acquisitions were averaged for each spectrum.

For the variable contact time (VCT) experiments, the contact times range from 0.01 to 60 ms, and 500 scans were averaged for each spectrum.

For the 2D-$^1H/^{13}C$ wideline separation spectra (WISE), the data matrix had a size of 64 points in t_1(^1H) dimension and 1024 complex data points in t_2(^{13}C) dimension. The spectral width in t_1 was

500 kHz (dwell time 2 μs) and 31250 Hz in t_2. The cross-polarization time was 1 ms. The dephasing experiments (nonquarternary suppression, NQS) were carried out by inserting a dephasing delay τ into the standard CP sequence following the cross-polarization and prior to acquisition. During this delay the dipolar decoupling is switched off. The signals of carbons with nearby protons vanishes due to dephasing, while the signals of quartenary carbons remain. For $\tau = 0$ μs, the dephasing experiment is identical to the standard CP/MAS.

RESULTS AND DISCUSSION

Cooling the melt, or precipitating from solution yields higher-ordered smectic-crystalline phases in the solid state for all the poly(ester imide)s is investigated in this article.[2,3,12,13] However, not all of the samples pass through a LC phase upon cooling. The PEI 1 with long spacers (n = 16, 22) crystallize directly from the isotropic melt, forming a spherulitic morphology.[18] The spherulites consist of a two-phase system with lamellae of 100–200 Å thickness, which gives rise to small-angle X-ray scattering. The crystal lamellae themselves contain a number of smectic layers. In contrast, the PEI 2 (n = 12, 16, 22) and PEI 3 (n = 12, 20) form monotropic smectic LC phases, which undergo a transition into the smectic-crystalline state upon further cooling. Rapid quenching of the isotropic phase or the LC melt below the glass-transition temperature freezes the smectic LC phase.

In order to determine the conformation of the spacers between the solid smectic layers of the mesogenic groups, all PEI 1, 2, and 3 were subjected to ^{13}C solid state NMR measurements with cross-polarization (CP), magic-angle spinning (MAS), and dipolar decoupling (DD) of the protons. Figure 2 represents the spectra of PEI 1, 2, and 3. The peak assignments are made on the basis of the additivity rules of substituents. The numbers on the peaks represent the carbon atoms as indicated in the chemical structures. The carbonyl-carbons show resonances at about 165 ppm, while those of the aromatic carbons occur between 110 and 140 ppm. The methylene carbons of the spacers are subject to the influence of substituent effects from the mesogen. The oxygen exerts a positive substituent effect (deshielding) of about +40 ppm on the α-carbon and about +5 ppm on the β-carbon. The shielding is enhanced in the γ position by −3 ppm. The inner δ-carbons of the spacers are influenced only by the conformation of their neighboring C—C-bonds. Under the conditions of magic-angle spinning and dipolar decoupling of the protons, the ^{13}C chemical shift provides infor-

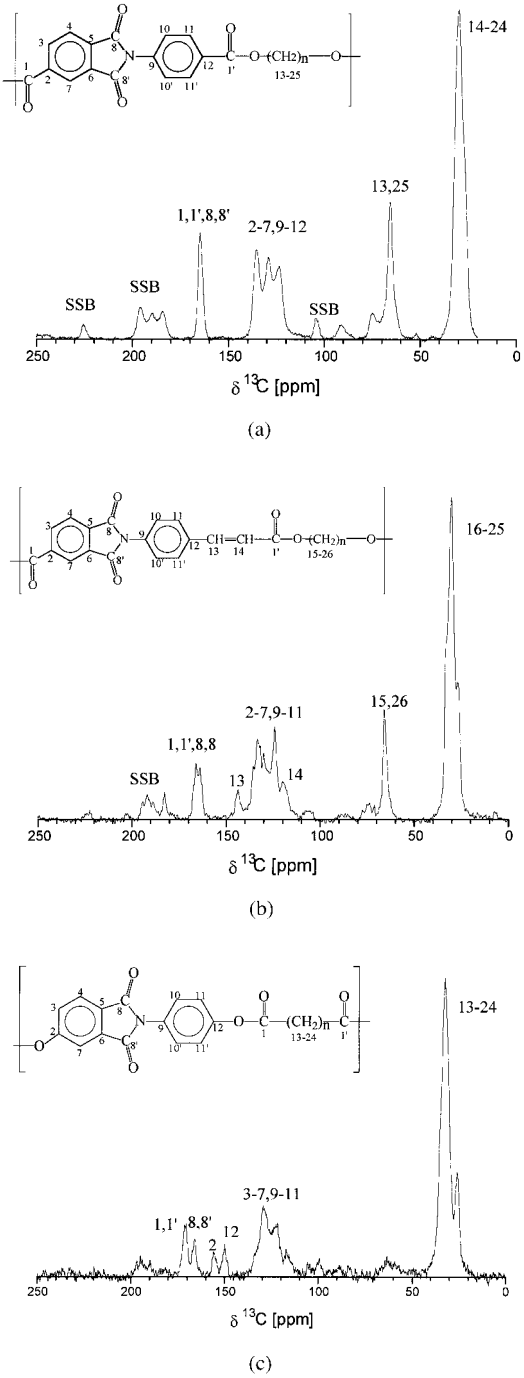

Figure 2. ^{13}C NMR CP/MAS spectra of PEI 1 (a), 2 (b), and 3 (c) at 20°C. The numbers in the spectra correspond to the numbers of the carbons in the chemical structure (see inset).

mation about the conformations of an alkane chain due to the γ-gauche effect.[16] The chemical shift of each methylene carbon is determined by the conformation of its two respective γ substituents. The gauche conformation exerts more shielding upon the carbon atom in γ position than the trans-conformation, and therefore, a conformational disorder in the alkane chain results in a downfield shift in the ^{13}C NMR resonance. At temperatures higher than the glass-transition of the alkyl chain, a C—C bond can be either ordered in trans-conformation (t) or disordered (d). In the latter case, the bond undergoes a rapid interconversion between the trans- and gauche conformation. In regard to the conformation of the respective two γ substituents, the carbons can be classified into three categories: tt, td, and dd. Since the trans and the gauche conformation are more or less equally populated in a disordered bond, and the shielding effect of a gauche conformation amounts approximately to 4 ppm, a disordered bond exerts a shielding of about 2 ppm on the adjacent carbon atom. Consequently, the tt-, td-, and dd-arrangements give rise to respective resonances at approximately 34, 32, and 30 ppm.

The ^{13}C chemical shift of the methylene carbons of several PEI samples is studied in order to determine the influence of temperature, spacer length, as well as chemical structure and packing of mesogenic groups on the conformational order of the spacers. The broad resonances of the methylene carbons in the different arrangements overlap in the region between 20 and 40 ppm. In the following, only this part of the spectra will be displayed as expanded plots. For an accurate evaluation of the peak positions and the peak intensities, a deconvolution into individual lines is performed. The thick, solid line represents the experimental data; the dotted line, the sum of the individual components giving the best fit; and the thin solid lines, the individual components. The line shape used for the individual components is a combination of Gaussian and Lorentzian functions. The peak position of each component provides the chemical shift which is related to the conformation by the γ-gauche effect.

Figure 3 represents the ^{13}C NMR CP/MAS spectra of PEI $\underline{1}$ (n = 12, 16, and 22) in the smectic-crystalline phase at 20°C. All spectra exhibit the signal of the γ-carbons at about 26.5 ppm. Its relative intensity decreases with increasing spacer length along with the fraction of γ-carbons in the spacer. The spectrum of PEI $\underline{1}$ n = 22 exhibits two additional signals. The sharp peak at 33.8 ppm indicates the presence of highly ordered trans–trans-conformations, while the broad one at 30.5 ppm has to be attributed to a disordered "dd"-arrangement of the spacer segments. The observed line shape and the concluded spacer conformation differ from those found by Cheng et al.[11] for smectic polyethers. Their investigations have shown mainly tt-conformations with small amounts of td-conformations in the smectic-crystalline state and a completely disordered dd-ar-

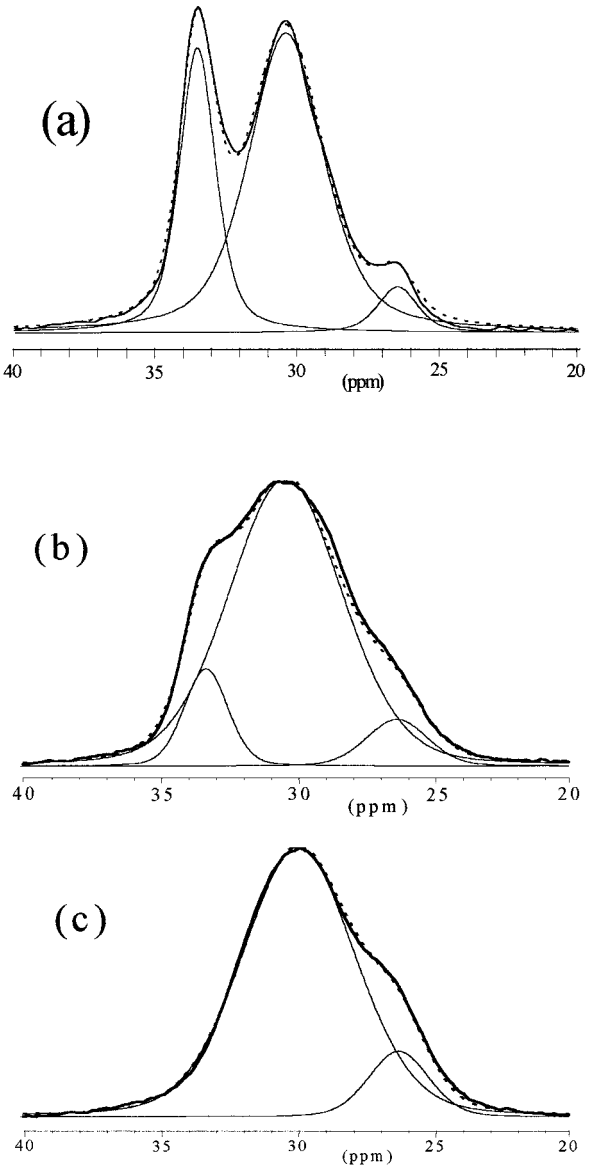

Figure 3. Expanded ^{13}C NMR CP/MAS spectra of PEI $\underline{1}$ n = 22 (a), 16 (b), and 12 (c) at 20°C. The thick full lines represent the experimental data; the thin full lines are the individual components of the deconvolution and the dotted line is the sum.

rangement only in the isotropic phase. However, in our case small angle X-ray scattering (SAXS) experiments[18] indicate the formation of a lamellar two-phase system during crystallization and the observed dd-arrangement can be attributed at least partly to the amorphous interlamellar regions.

In Figure 4 the comparison of the spectra of PEI 1 n = 22 (a), 16 (b), and 12 (c) reveals a strong influence of the spacer length upon the conformation. While the tt-signal is detectable in PEI 1 (n = 16) as a shoulder at 33.5 ppm, the PEI 1 (n = 12) exhibits only one broad resonance with a maximum at 30.5 ppm for the inner δ-carbons. Obviously, the conformational order of the spacers increases with the number of methylene groups.

The same relationship is found in the spectra of PEI 2 (n = 12, 16, and 22) depicted in Figure 4. The intensity of the tt-signal at about 33.5 ppm increases likewise with the number of methylene groups in the spacer. But in contrast to PEI 1, contributions of a td-component have to be considered to obtain a satisfactory fit of the PEI 2 spectra, in particular for n = 22. Once again, the components at about 30 ppm indicate that major parts of the spacer segments are in a disordered dd-arrangement typical for the amorphous phase. Although the PEI 2 (n = 12, 16, 22) pass through a smectic LC phase upon cooling, SAXS experiments indicate that a lamellar two-phase system is formed during the transition into the smectic-crystalline state as in PEI 1.

Furthermore, the comparison of the spectra of PEI 1 and PEI 2 with identical spacer lengths indicates that PEI 2 has generally a higher tendency to form trans-conformations than PEI 1. This observation will be discussed later based on a quantitative analysis.

For the PEI 3, this tendency is even more marked. The ^{13}C NMR CP/MAS spectrum of PEI 3 (n = 20) in Figure 5a exhibits the most intense peak at 33.4 ppm which can be attributed to the tt-arrangement of the spacer segments. In contrast, the td-peak at 32.0 ppm and the dd-signal at 30.2 ppm are much weaker. It should be pointed out that the resonances become broader with increasing disorder in the respective arrangements. While the tt-components exhibit half widths of about 100 Hz, the dd-signals are about 200 Hz wide. The spectrum of PEI 3 (n = 12) [Fig. 5b] displays a broad peak at 32.4 ppm which may cover the two unresolved resonances of the tt- and td-arrangements. The signal of the dd-component at 30.0 ppm is very weak. In both spectra of PEI 3 the resonance signals of the β-carbons are recognizable as shoulders at 35.5 ppm in addition to the resonances of the γ-carbons at 26.2 ppm.

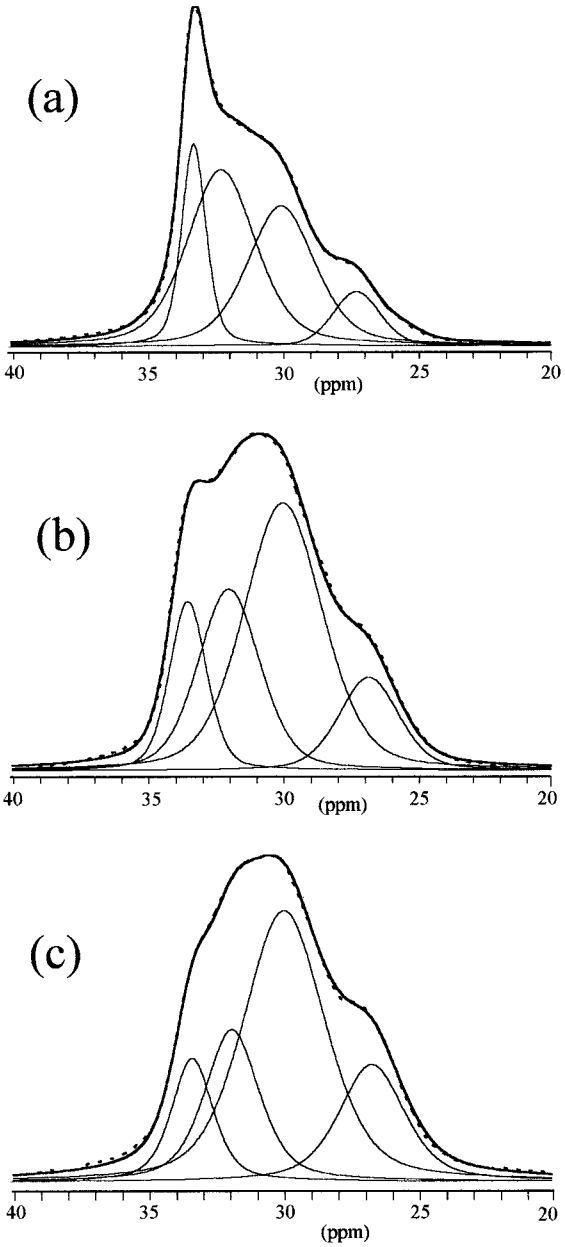

Figure 4. Expanded ^{13}C NMR CP/MAS spectra of PEI 2 n = 22 (a), 16 (b), and 12 (c) at 20°C. The thick full lines represent the experimental data; the thin full lines are the individual components of the deconvolution and the dotted line is the sum.

We will now attempt a quantitative analysis of the conformational order in the spacers based on the chemical shift and the intensity of the resonance signals of the individual components. However, the signal intensities of CP spectra are not

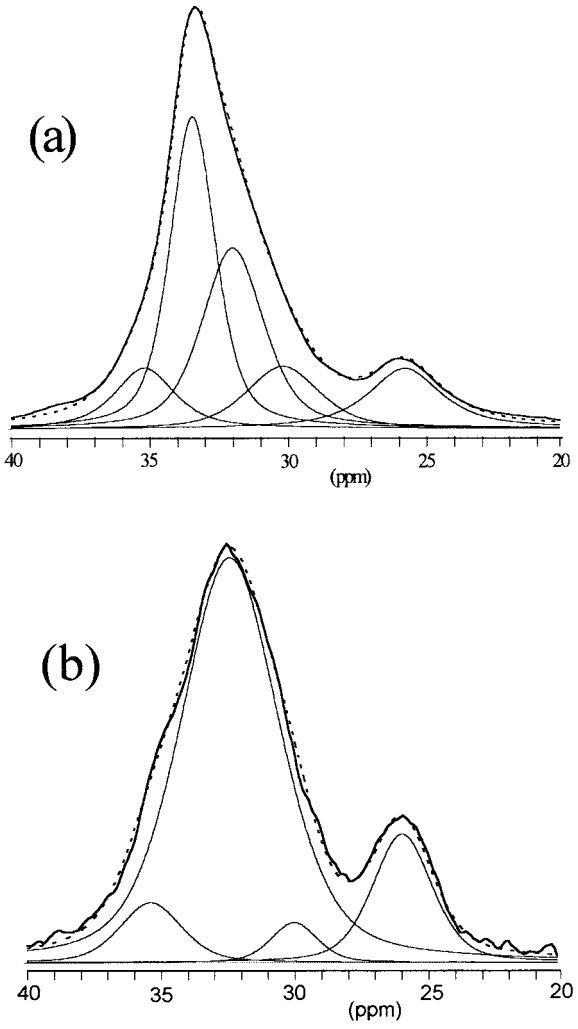

Figure 5. Expanded ^{13}C NMR CP/MAS spectra of PEI 3 $n = 20$ (a), and 12 (b) at 20°C. The thick full lines represent the experimental data; the thin full lines are the individual components of the deconvolution and the dotted line is the sum.

exactly proportional to the fraction of the corresponding nuclei due to different CP sensitivities.[19,20] Based on variable contact time experiments, the relationship between signal intensity and contact time in eq. (1) can be used to calculate the maximum attainable signal intensity which is proportional to the spin population:

$$M_C = M_C \exp(-\tau/T_{1\rho}(^1H))[1 - \exp(-\tau/T_{CH})] \quad (1)$$

In eq. (1), τ is the contact time, M_C the signal intensity at τ, and M_C the maximum static magnetization which is related to the number of resonant spins. T_{CH} is the cross-polarization time constant, and $T_{1\rho}(^1H)$ is the proton spin relaxation time in the rotating frame. Eq. (1) is a simplified form of the equation which relates signal intensity and contact time. It is assumed that $T_{1\rho}(^1H) \gg T_{CH}$.

It turns out that eq. (1) gives an excellent fit of the VCT curves for the signals of the carbonyl and aromatic carbons, but not for the resonances of the methylene carbons. As an example, Figure 6 depicts the intensity of the "dd"-peak at 30.9 ppm of PEI 1 ($n = 16$) at 20°C as a function of the contact time τ in a semi-logarithmic plot. The circles represent the experimental data and the dotted line represents the best fit from eq. (1). The deviation is severe although the assumption $T_{1\rho}(^1H) \gg T_{CH}$ is proven correct. In particular, the increasing magnetization at short delays cannot be fitted satisfactorily. For the next approximation, one can assume bimodal cross-polarization kinetics with two time constants which differ by more or less one decade. The full line in Figure 6 represents the best fit resulting from eq. (2) which contains two cross polarization times T_{CH1} and T_{CH2}.

$$M_C = M_{C0} \exp(-\tau/T_{1\rho}(^1H))[1 - w_1 \times \exp(-\tau/T_{CH1}) - (1 - w_1)\exp(-\tau/T_{CH2})] \quad (2)$$

As one can see, the introduction of the second cross-polarization time improves the fit significantly. Essentially the same course of magnetization is found for other samples and at different temperatures. T_{CH1} is of the order of 0.03 ms with a fraction of about 0.6 and T_{CH2} ranges between 0.2 and 1 ms. It can be assumed that the two components also have different relaxation times,

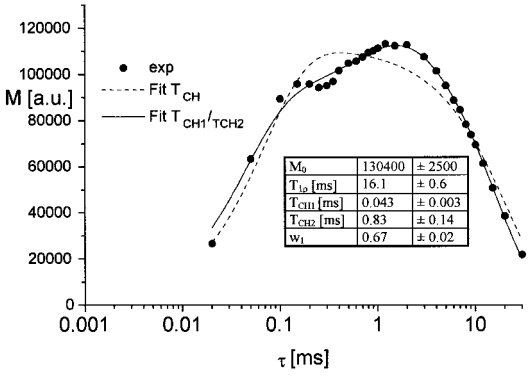

Figure 6. Magnetization M of the "dd"-component at 30.9 ppm in the ^{13}C NMR CP/MAS spectrum of PEI 1 ($n = 16$) at 20°C as a function of the contact time τ. The circles represent the experimental data, the dotted line is the best fit from eq. 1 and the full line is the fit from eq. 2. The inset lists the resulting parameters.

but obviously their deviation is too small to justify the assumption of a second $T_{1\rho}(^1H)$.

The observed heterogeneity in the relaxation behavior has been confirmed by ^2H NMR measurements on different samples of PEI 1, which were deuteriated selectively in the central spacer segments. They also reveal a biexponential longitudinal relaxation and the two resulting spin-lattice relaxation times T_1 differ by one decade.[21] As mentioned above, these polymers form a two-phase system of crystalline lamellae and amorphous regions. But this fact cannot explain the bimodal cross-polarization behavior of the methylene carbons because the different degrees of order in the two phases would account for the spacers as well as for the mesogens. As stated above, the VCT-curves of their respective signals are monomodal. In addition, PEI 2 samples have been quenched from the melt resulting in a frozen smectic LC glass which show no small angle X-ray scattering. Nevertheless, bimodal cross-polarization kinetics is observed for the methylene carbons once again.

The variation of the magnetization at short delays could also be interpreted as oscillations, which have been previously observed for other polymers.[22,23] These oscillations have been explained by a coherent energy transfer and Ernst et al.[24] derived an equation which describes the cross-polarization of an isolated spin pair, but it does not fit satisfactorily to our experimental data assuming only one cross-polarization component.

However, the distinction of two cross-polarization components or the observed oscillations do not influence the M_{C0} values and the quantitative conformational analysis significantly and, therefore, these observations do not have to be discussed conclusively at this point. Table I lists typical values of $T_{1\rho}(^1H)$, T_{CH1}, and its fraction w_1 and T_{CH2} for PEI 1, 2, and 3 with different spacer lengths at different temperatures for the tt-, td-, and dd-signals which occur at about 33.5, 32.0, and 30.5 ppm, respectively. One can see that the condition $T_{1\rho}(^1H) \gg T_{CH}$ is fulfilled. $T_{1\rho}(^1H)$ is of the order of 7 to 25 ms and becomes shorter with increasing temperature. It can be concluded that the motions which are associated with $T_{1\rho(H)}$ (kilohertz range) are relatively slow, so that $\omega_0^2\tau_C^2 > 1$, in which ω_0 is the lamor frequency and τ_C is the correlation time of the motion. Although the spacer segments may be mobile, the sample is solid from the NMR point of view, because the relaxation of the protons in the spacers and in the mesogens is averaged to a large extent by spin diffusion. In general, one observes shorter relaxation times for the dd-arrangement than for the tt-conformations which proves the increased mobility in the disordered segments.

As mentioned above, a quantitative conformational analysis can be made based on the chemical shift values of the individual components after deconvolution and their intensities corrected by the VCT experiments. Table II lists the chemical shifts and the relative intensities of the tt, td, and dd-peaks of PEI 1, 2, and 3 with different spacer lengths and at different temperatures. The conformational order of the spacers, ρ, can be empirically defined by the following expression proposed by Cheng et al.[11]:

$$\rho = I_{tt}F_{tt} + I_{td}F_{td} + I_{dd}F_{dd} \qquad (3)$$

I_{tt}, I_{td}, and I_{dd} are the corrected relative signal intensities for the methylene carbons in the tt, td, and dd-arrangements. F_{tt}, F_{td}, and F_{dd} are weight factors based on the observed chemical shift values of the tt-, td-, and dd-peak in relation to the chemical shift of perfectly ordered crystalline alkane chains δ_{cryst} and the completely disordered melt δ_{melt} defined in eq. (4).

$$F = \frac{\delta - \delta_{melt}}{\delta_{cryst} - \delta_{melt}} \qquad (4)$$

Since the poly(ester imide)s do not form a three-dimensional crystalline phase nor melt within the temperature range accessible by the used probe head, the values of polyethylene crystals δ_{cryst} = 34.0 ppm and of the amorphous phase δ_{melt} = 30.0 ppm were used. This is a crude approximation but it allows at least the comparison of the conformational order in different samples and phases.

The comparison of the ρ-values in Table II indicates clearly that the conformational order in the spacers increase with increasing spacer length. Due to the larger number of C—C-bonds, the longer spacers have more rotational isomeric conformers and, therefore, can form the energetically more favorable tt-conformations. The shorter spacers, on the other hand, are forced to adopt larger amounts of gauche conformations due to the molecular constrains caused by their anchoring to the rigid mesogen layer. In other words, the occurance of tt-conformations is a result of conformational freedom.

Table I. Position $\delta^{13}C$, Relaxation Time $T_{1\rho}(^1H)$, Cross Polarization Times T_{CH1} and T_{CH2} and Their Fraction w_1 of the tt-, td-, and dd-peaks of PEI 1, 2, and 3 with Different Spacer Lengths n at Different Temperatures

Sample	Peak	Temp. [°C]	$\delta^{13}C$ [ppm]	$T_{1\rho}(^1H)$ [ms]	T_{CH1} [ms]	T_{CH2} [ms]	w_1
PEI 1 (n = 22)	tt	20	33.9	22	0.034	0.32	0.62
	tt	60	33.6	20.1	0.032	0.66	0.74
	tt	100	33.7	13.6	0.028	0.4	0.6
	dd	20	30.7	16.0	0.025	0.70	0.58
	dd	60	30.7	9.2	0.06	0.89	0.67
	dd	100	30.7	9	0.047	0.78	0.47
PEI 1 (n = 16)	tt	20	33.8	23.7	0.019	0.17	0.6
	tt	60	33.9	20.1	0.023	0.19	0.7
	tt	100	33.9	13.2	0.018	0.36	0.6
	dd	20	30.9	16.1	0.043	0.83	0.68
	dd	60	30.7	9.3	0.04	0.57	0.53
	dd	100	30.6	6.2	0.06	0.57	0.55
PEI 2 (n = 22)	tt	20	33.8	16.2	0.03	0.37	0.68
	tt	60	33.6	16.7	0.024	0.28	0.65
	tt	100	33.4	13.6	0.027	0.26	0.71
	td	20	32.1	13.5	0.047	0.81	0.73
	td	60	32.1	12	0.032	0.64	0.65
	td	100	32.1	10.1	0.032	1.74	0.53
	dd	20	30	17.2	0.056	1.28	0.77
	dd	60	30.3	11.1	0.027	0.6	0.4
	dd	100	30.3	8.8	0.034	0.57	0.38
PEI 2 (n = 16)	tt	20	33.7	22.0	0.028	0.35	0.73
	tt	60	33.9	18.7	0.023	0.33	0.69
	tt	100	33.7	11.5	0.026	0.34	0.65
	dd	20	31.0	13.8	0.040	0.81	0.67
	dd	60	31.1	11.5	0.040	0.71	0.62
	dd	100	31.0	5.8	0.047	0.62	0.62
PEI 2 (n = 16)	td	20	31.6	10.5	0.039	0.87	0.66
Quenched	dd	20	29.6	12.6	0.035	0.3	0.74
PEI 3 (n = 22)	tt	20	33.5	30.6	0.027	0.25	0.58
	tt	60	33.5	25.1	0.027	0.31	0.68
	tt	100	33.5	23.5	0.027	0.28	0.66
	dd	20	31.4	16.4	0.051	0.85	0.66
	dd	60	31.2	9.4	0.046	0.86	0.6
	dd	100	30.8	8.8	0.052	0.99	0.55

Furthermore, the quantitative analysis proves the above-mentioned influence of the mesogen type on the spacer conformation. For identical numbers of methylene groups, the spacers of the PEI 2 exhibit a higher conformational order than those in PEI 1. This observation cannot be explained straightforwardly by the molecular geometry of the repeating units, because the introduction of the planar trans-substituted ethenyl group of the cinnamic acid in PEI 2 does not change the direction of the spacer bonding, as compared to PEI 1, in contrast to the different conformational order resulting from ester- and ether-linkage studied by Yoon et al.[25] in nematic systems. Moreover, it can be assumed that a relationship exists between the packing of the mesogens within the smectic layers the spacer conformation. As demonstrated by X-ray fiber patterns, the PEIs 1 exclusively form smectic phases in which the mesogens are oriented perpendicularly with respect to the layer plane, namely a higher-ordered smectic-E phase in the solid state.[26] Whereas, in the PEIs 2, the mesogens are inclined at an angle of about 40° with respect to the normal of the layers, so that a smectic-H phase is formed.[27] Obviously, this staggered arrangement of the mesogenic groups and the resulting jut of the neighboring mesogen favor a largely extended conformation of the spacer. This assumption is supported by the observation that PEI 2 n = 10 also forms a tilted

Table II. ^{13}C NMR CP/MAS Results of the Methylene Carbons in PEI 1, 2, and 3 with Different Spacer Length n at 20°C

Sample	δ_{tt} [ppm]	I_{tt}	δ_{td} [ppm]	I_{td}	δ_{dd} [ppm]	I_{dd}	ρ
PEI 1 n = 22	33.81	0.18	33.0	0.07	31.0	0.76	0.40
n = 16	33.47	0.10	—	—	30.50	0.90	0.20
n = 12	—	—	—	—	30.16	1.0	0.04
PEI 2 n = 22	33.29	0.19	32.28	0.46	30.08	0.36	0.42
n = 16	33.55	0.16	32.04	0.29	30.03	0.55	0.30
n = 12	33.43	0.14	32.00	0.23	30.03	0.62	0.24
n = 16(q)	—	—	32.10	0.61	30.08	0.39	0.32
PEI 3 n = 20	33.44	0.48	32.00	0.37	30.20	0.15	0.60
n = 12	—	—	32.42	0.94	30.03	0.04	0.57
n = 12(q)	—	—	32.27	0.82	30.64	0.18	0.50

(q) indicates samples quenched into the frozen LC-phase.

smectic phase and still exhibits a tt-signal, whereas, in the case of n = 9, an upright mesogen orientation and no tt-conformations are found. In PEI 3 n = 12 and 20, the conformational order parameter ρ is even higher than in PEI 1 and 2 (see Table II). The main reason for this improved conformational order of the spacers in average, is the low amount of the dd-conformations. It can be concluded that the interlamellar regions are either relatively small or contain a liquid-crystalline order rather than an amorphous state.

On one hand, the X-ray fiber patterns of the smectic crystalline phase show again that a tilted smectic-H phase is formed,[28] as in PEI 2. On the other hand, the carboxylate group is reversed compared to PEI 1, and the formation of highly extended conformers in spacers, which are appended via mesogen (—O—CO—) spacer linkages, is in agreement with the calculations of Yoon et al.[25]

Taken together, it can be concluded that the formation of the trans–trans sequences in the spacers in the smectic-crystalline phase is favored by an increasing spacer length and by a staggered packing of the mesogens.

Unfortunately, for the PEI investigated here, the spacer conformation in the smectic LC phase cannot be studied *in situ,* because the transition temperatures exceed the service temperature of the probe head. Therefore, the LC phase was quenched rapidly below T_g and afterwards the conformational order of the resulting smectic LC glass was measured by ^{13}C NMR CP/MAS spectroscopy. Figure 7 displays the spectra of PEI 2 (n = 16) in the smectic-crystalline state (a) and in the frozen smectic LC-phase (b) at 20°C. The comparison indicates that the signal of the tt-arrangement vanishes completely in the LC phase, but in return the td-peak becomes dominating. Furthermore, a sizable amount of the dd-component remains. These observations agree with the

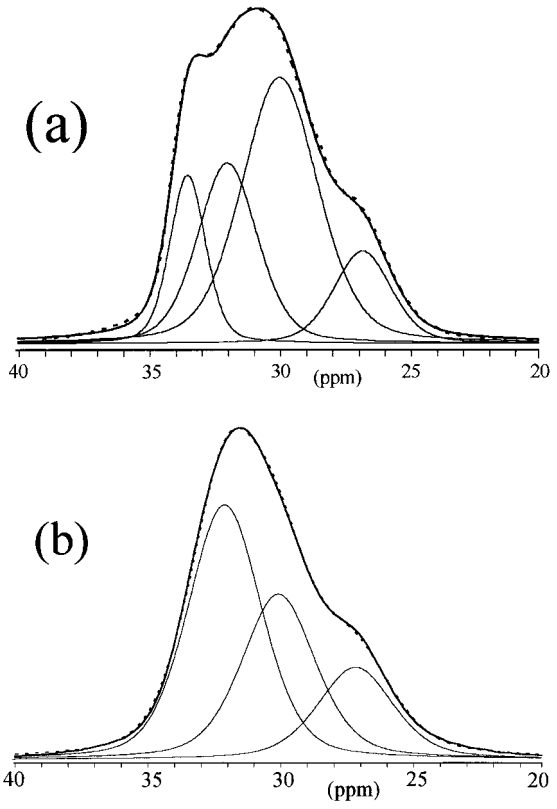

Figure 7. Expanded ^{13}C NMR CP/MAS spectra of PEI 2 n = 16 at 20°C in the smectic-crystalline phase (a) and in the frozen smectic LC-phase (b). The thick full lines represent the experimental data; the thin full lines are the individual components of the deconvolution and the dotted line is the sum.

results published by Cheng et al.[11] for a smectic LC phase (S_F) of polyethers. However, our quantitative analysis reveals that the order parameters ρ of the smectic-crystalline and the frozen LC phase are the same within the error limit. During crystallization, the tt-signal occurs at the expense of the td-peak, but the amount of dd-conformations increases in the same magnitude. This observation can be explained by the mechanism of crystallization from the LC phase based on X-ray scattering results.[29] In the course of crystallization from the LC phase, a small-angle X-ray reflection develops, which indicates the formation of a lamellar two-phase system with a long period of about 200 Å. While the molecular order is increased within the growing smectic-crystalline lamellae, the smectic layer structure is lost in the regions between the lamellae.

Thermal Stability and Localization of the tt-Conformations

The existence of trans–trans conformations within the spacer layer can be explained in principle by assuming two different models represented schematically in Figure 8. In the cluster model [Fig. 8(a)], the tt-conformations are embedded within a crystallike ordered domain due to lateral interactions, whereas in the rope model [Fig. 8(b)], the spacers are largely extended and braced between the rigid mesogen layers. In the following, these models will be discussed on the basis of the thermal stability, mobility, and localization of the trans–trans-sequences.

The ^{13}C NMR CP/MAS spectra of different PEI samples at elevated temperatures indicate a remarkable thermal stability of the tt-conformations in the spacers in the smectic crystalline phase. As an example, Figure 9 depicts the ^{13}C NMR CP/MAS spectra of PEI $\underline{2}\,n = 22$ at different temperatures. On the one hand, the resonance of the dd-arrangement at 30.5 ppm becomes narrower and increases significantly. On the other hand, the signal of the tt-conformations at 33.5 ppm persists up to 150°C. At temperatures higher than 120°C the signal of the γ-carbons at about 27 ppm is split into two components. The development of the component with high-field shift indicates increasing disorder in the γ position. The quantitative analysis of the individual components from the deconvolution, represented in Table III, reveals that the fraction of the dd-component increases at the expense of the td-component, while the amount of tt-conformations remains virtually constant. The resulting order, parameter ρ, decreases from 0.42 at 20°C to 0.25 at 150°C; that is, merely 20°C below the melting point of the polymer. This behavior was found to be essentially the same for all samples.

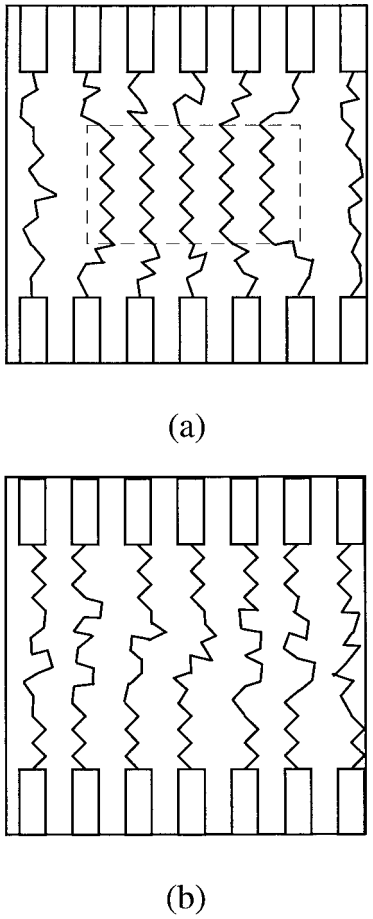

Figure 8. Schematic representation of two models for the arrangements of tt-conformations.

The observed thermal stability of the tt-conformations is the first piece of evidence, that they are not part of a nano-crystal within the spacer layer. Such ordered crystal-like structures have been found for alkane side chains of hairy-rod-type molecules which form so-called sanidic or biaxial-nematic layer structures.[15] In these structures, the rigid main chains form a back-to-back array, while the alkane side chains interdigitate forming a paraffin layer. Since the side chains are fixed only at one end, they possess enough conformational freedom to form nano-crystals by a parallel packing of all-trans sequences due to lateral van-der-Waals interactions. Upon heating, these nano-crystals undergo a reversible melting, indicated by a sudden disappearance of the trans–

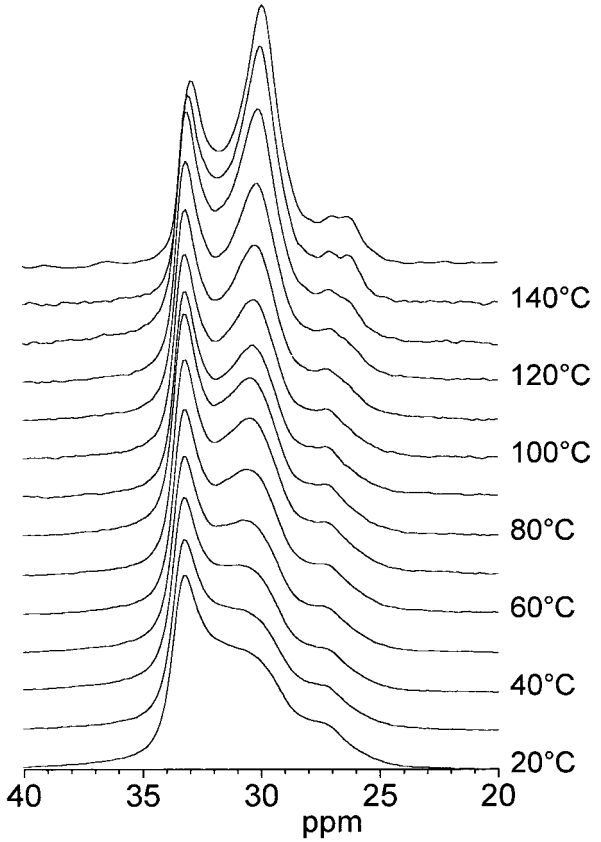

Figure 9. ^{13}C NMR CP/MAS spectra of PEI 1 $n = 22$ at different temperatures.

trans signal in the ^{13}C CP/MAS NMR spectra and an endothermal peak in the differential scanning calorimetry (DSC) at 40–50°C. This melting temperature is approximately 30°C higher than the T_m of the free n-alkane, because the chains are appended to the rigid array of aromatic main chains. However, no such transition has been observed for main-chain polymers up to 100°C and, therefore, the ordering of the alkane chains due to lateral enthalpic interactions is unlikely.

More information about the nature of the trans–trans conformations may be derived from 2D $^{13}C/^{1}H$-WISE NMR spectra which relate structure and mobility of molecular moieties.[30,31] The line width of the ^{1}H wideline spectrum characterizes the strength of the dipolar coupling among protons and, thus, the molecular mobility. The WISE spectra of PEI 2 $n = 22$ (Fig. 10) at 20°C (a), and 100°C (b), are examples which exhibit the signal of the tt-conformations in the carbon dimension at about $\delta^{13}C = 33.5$ ppm, and also, the one resulting from the dd-arrangement at about $\delta^{13}C = 30.5$ ppm. The ^{1}H line width of the tt-signal (44 kHz), and the dd-signal (28 kHz), do not differ very much, which indicates a comparable mobility for all spacer segments irrespective of the conformation, in agreement with the observed $T_{1\rho(H)}$ values (Table I). The ^{1}H half-widths differ from the values measured for crystalline (75 kHz) and noncrystalline (5 kHz) regions in polyethylene.[32] On the one hand, the tt-conformations in the spacers are too mobile to presuppose a crystal-like lateral ordering in domains. On the other hand, the disordered segments of the spacers exhibit a restricted mobility compared to the coiled alkane chain which is due to molecular constrains. During heating the ^{1}H line widths of the tt and the dd signal decrease in the same manner indicating that the whole spacer gains mobility. Unfortunately, the distances between the carbons

Table III. ^{13}C NMR CP/MAS Results of the Methylene Carbons in PEI 2 ($n = 22$) at Different Temperatures

T [°C]	δ_{tt} [ppm]	I_{tt}	δ_{td} [ppm]	I_{td}	δ_{dd} [ppm]	I_{dd}	ρ
20	33.30	0.19	32.28	0.46	30.06	0.36	0.42
30	33.30	0.18	32.28	0.46	30.05	0.37	0.41
40	33.32	0.19	32.33	0.43	30.13	0.38	0.42
50	33.29	0.20	32.27	0.42	30.16	0.38	0.42
60	33.26	0.19	32.33	0.36	30.24	0.44	0.39
70	33.30	0.19	32.40	0.35	30.24	0.44	0.39
80	33.27	0.22	32.31	0.34	30.26	0.44	0.40
90	33.25	0.19	32.38	0.34	30.22	0.47	0.38
100	33.26	0.20	32.38	0.31	30.24	0.49	0.37
110	33.22	0.19	32.38	0.29	30.18	0.52	0.35
120	33.22	0.17	32.38	0.31	30.15	0.52	0.34
130	33.15	0.17	32.26	0.33	30.10	0.50	0.33
140	33.12	0.13	32.30	0.30	30.02	0.57	0.28
150	33.00	0.16	32.0	0.26	30.00	0.58	0.25

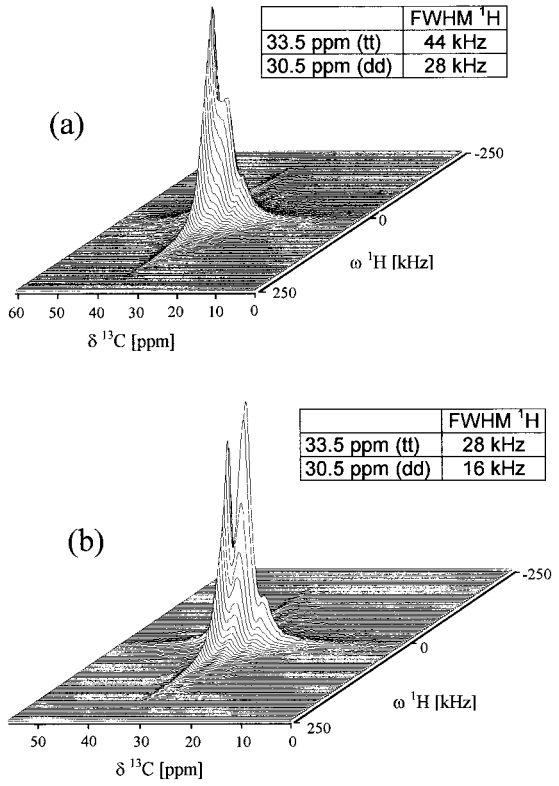

Figure 10. $^{13}C/^{1}H$ WISE NMR spectra of PEI 2 ($n = 22$) at 20°C (a) and 100°C (b).

which respectively contribute to the tt and the dd signals may be so short that the influence of spin diffusion cannot be excluded for certain. It may partly average the proton line widths of neighboring tt and dd sequences.

In order to investigate the dynamics of the spacers in more detail, analogous PEI 1 have been synthesized in which the four central spacer segments are deuteriated.[26] The ^{2}H NMR spectra reveal that rapid motions of the spacers start at −100°C, and the central segments are already highly mobile at ambient temperature. Once again, this observation contradicts the model of crystallike packing of the spacer segments. However, the investigation of the segmental mobility in the spacers by means of ^{2}H NMR spectroscopy is the subject of another article.[21] Moreover, in these specifically deuteriated analogous PEIs, the position of the trans−trans conformations can be localized precisely by a proton attachment test in the ^{13}C NMR CP/MAS spectroscopy using a dephasing delay.[33] The only difference from the standard CP pulse sequence is that, following the CP step, the dipolar decoupling is switched off for a time (τ). The ^{13}C signal is then recorded in the usual way. In this dipolar dephasing experiment, the signal intensity decreases with increasing delay τ, depending on the strength of the dipolar interaction between the ^{13}C and ^{1}H. This dipolar interaction is proportional to the number of interacting protons, dependent on the internuclear distance, and inversely related to the rate of motion. According to the number of bonded protons and their mobility, the ^{13}C atoms can be classified into three categories: (1) the signals of rigid, highly protonated ^{13}C will have already been suppressed by a short delay τ, due to their short spin-spin relaxation time, (2) signals of mobile, protonated carbons will be suppressed to a lesser extent because the local dipolar field is weaker, due partly to motional averaging and a longer relaxation time, and (3) signals of nonprotonated ^{13}C will be affected at least by the larger distance to the nearest neighboring protons. After a dephasing delay of $\tau \approx 50$ μs, the signals of the carbons with adjacent protons will be suppressed (nonquarternary suppression, NQS) and only the quarternary carbons will be detected, which are the four deuteriated central-methylene groups in this case.

Figure 11 depicts NQS spectra of PEI 1 ($n = 22$) with different dephasing delays (τ). With increasing delay, the tt-resonance at 33.5 ppm disappears more and more compared to the dd-signal at 30.5 ppm, clearly demonstrating that the central spacer segments do not contain tt-conformations. Consequently, they must be localized in the outer parts of the spacer. It can be concluded that the formation of trans−trans conformations is induced by the rigidity of the mesogens, but their molecular motion is not restricted by lateral interactions with neighboring spacer segments. Hence, the rope-model in Figure 8b is much more likely to describe the spacer conformations between the smectic PEI layers, even for long spacers, because the model is consistent with the observed thermal stability of the tt-conformations, the absence of a DSC melting endotherm at 40−100°C, and the more or less uniform mobility from the WISE experiments and the NQS results.

Copolymers with Different Spacer Lengths

Another interesting question concerns the spacer conformation in a random copolymer with two different spacer lengths. If the smectic-layer structure is retained despite the random sequence, both spacers are embedded within the same layer structure. It can be assumed, that the length of

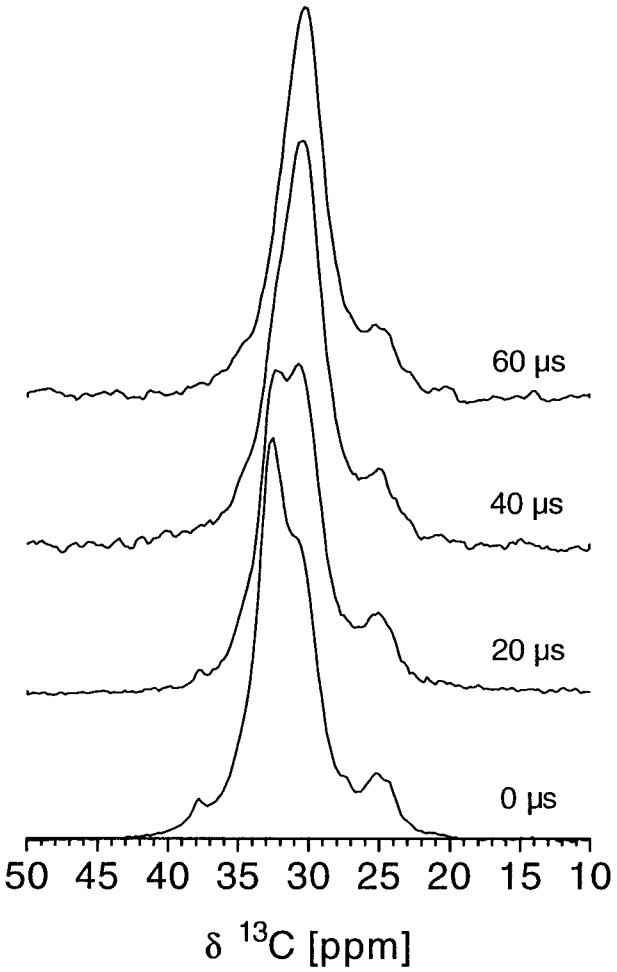

Figure 11. ^{13}C NMR spectra of PEI 1 $n = 22$ at 60°C with different dephasing delays τ.

the short spacer limits the layer spacing. Furthermore, the volume requirements of the long spacer should favor an extension of the short spacer. A random copoly(ester imide) 1 has been synthesized containing dodecane ($n = 12$) and docosane ($n = 22$) spacers in 50/50 mole composition. In fact, the X-ray measurements of this co-PEI 1 $n = 12/22$ indicate that its d-spacing of 30 Å is slightly larger than the layer distance of the homopolymer PEI 1 $n = 12$ (28 Å). Unfortunately, the conventional conformation analysis via the γ-gauche effect from the ^{13}C CP/MAS spectra cannot distinguish the two different spacers in the copolymer. It only provides information about the averaged conformation of the short spacer which may be more extended, and the long spacer which should adopt a more coiled conformation. Again, the required selectivity can be achieved by dephasing delay experiments (NQS) on partly deuteriated samples. A random co-PEI 1 n = D12/22 (50 : 50 mol %) was synthesized in which only the four central segments of the dodecane spacer ($n = 12$) are deuteriated (Fig. 12). A dephasing delay of $\tau > 50$ μs suppresses the signals of the outer protonated segments of the dodecane spacer and those of the protonated $n = 22$ spacer. The comparison depicted in Figure 13 of the CP/MAS spectrum of the $n = 12$ homopolymer (a), with the NQS spectrum of co-PEI 1 n = D12/22 (b), proves the supposed extension of the dodecane spacer in the copolymer. The main resonance signal exhibits a downfield-shift (deshielding) of 1.3 ppm so that it can be rather attributed to a td-than to dd-arrangement. In addition, the new signal at 34 ppm, indicates that in the copolymer, even the central spacer segments are forced, at least, in part, to adopt trans–trans conformations.

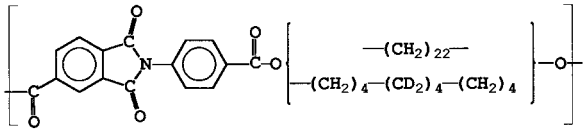

Figure 12. Chemical structure of co-PEI 1 n = D12/22 with selectively deuteriated dodecane spacer.

CONCLUSIONS

^{13}C solid state NMR employing magic-angle spinning and dipolar proton decoupling can be utilized to investigate the conformation of alkyl spacers

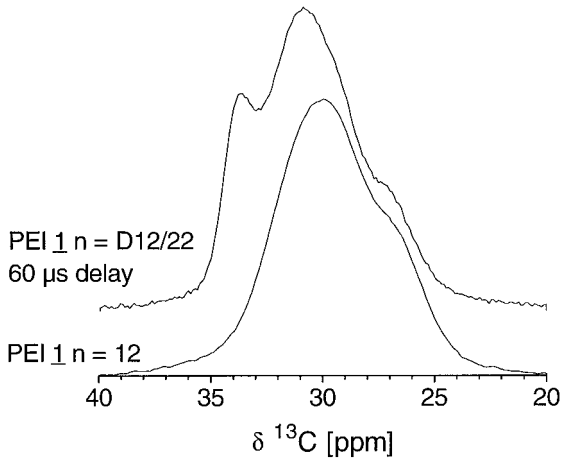

Figure 13. Comparison of the ^{13}C CP/MAS spectrum of PEI 1 ($n = 12$) (a) and the dephasing delay spectrum ($\tau = 60$ μs) of co-PEI 1 n = D12/22 (b) at 20°C.

via the γ-gauche effect. While the frozen liquid-crystalline state is characterized mainly by alternating sequences of ordered and disordered segments "td", the smectic-crystalline phase contains major sequences in trans–trans conformation. The amount of tt-conformations increases with the spacer length of the polymer. The thermal stability and the dynamics of the trans–trans-conformations in the spacers between the smectic layers indicate that this ordering is caused by the rigidity of the mesogens and not the lateral interactions of the spacers. The all-trans sequences are located in the outer parts of the spacer, and their mobility is restricted in comparison to the inner disordered conformations due to the anchoring to the rigid mesogen layer. The chemical structure of the mesogen, and the resulting packing within the smectic layer, exert a profound influence on the spacer conformation. The staggered, resp. tilted arrangement of the mesogens in a smectic-H phase exerts less constrains upon the spacer conformation than the orthogonal orientation in the smectic-E phase.

In a random copolymer containing two different spacer lengths, the short spacers are stretched into a more extended conformation than in the corresponding homopolymer, while the long spacers adopt a coiled conformation.

The authors thank Prof. H. R. Kricheldorf for providing the samples synthesized by Dr. N. Probst.

REFERENCES AND NOTES

1. Y. Yoon, R. Ho, B. Moon, D. Kim, K. W. McCreight, F. Li, F. W. Harris, S. Z. D. Cheng, V. Percec, and P. Chu, *Macromolecules,* **29,** 3421 (1996).
2. J. de Abajo, J. de la Campa, H. R. Kricheldorf, and G. Schwarz, *Makromol. Chem.,* **191,** 537 (1990).
3. H. R. Kricheldorf, G. Schwarz, J. de Abajo, and J. de la Campa, *Polymer,* **32,** 942 (1991).
4. S. D. Hudson, A. J. Lovinger, R. G. Larson, D. D. Davis, R. O. Garay, and K. Fujishiro, *Macromolecules,* **26,** 5643 (1993).
5. J. Watanabe and M. Hayashi, *Macromolecules,* **21,** 278 (1988).
6. S. Z. D. Cheng, Y. Yoon, A. Zhang, E. P. Savitski, J. Park, P. Chu, and V. Percec, *Macromol. Rapid Commun.,* **16,** 533 (1995).
7. R. Pardey, A. Zhang, P. A. Gabori, F. W. Harris, S. Z. D. Cheng, J. Adduci, J. V. Facinelli, and R. W. Lenz, *Macromolecules,* **25,** 5060 (1992).
8. J. Leisen, C. Boeffel, H. W. Spiess, D. Y. Yoon, M. H. Sherwood, M. Kawasumi, and V. Percec, *Macromolecules,* **28,** 6937 (1995).
9. S. Brukner, J. C. Scott, D. Y. Yoon, and A. C. Griffin, *Macromolecules,* **18,** 2709 (1985).
10. J. Cheng, Y. Jin, B. Wunderlich, S. Z. D. Cheng, M. A. Yandrasits, A. Zhang, and V. Percec, *Macromolecules,* **26,** 5991 (1992).
11. J. Cheng, Y. Yoon, R.-M. Ho, M. Leland, M. Guo, S. Z. D. Cheng, P. Chu, and V. Percec, *Macromolecules,* **30,** 4688 (1997).
12. H. R. Kricheldorf, N. Probst, and C. Wutz, *Macromolecules,* **28,** 7990 (1995).
13. H. R. Kricheldorf, N. Probst, G. Schwarz, and C. Wutz, *Macromolecules,* **29,** 4234 (1996).
14. W. L. Earl, and D. L. VanderHart, *Macromolecules,* **12,** 762 (1979).
15. A. Whittaker, U. Falk, and H. W. Spiess, *Makromol. Chem.,* **190,** 1603 (1989).
16. E. Tonelli, Ed., *NMR-Spectroscopy and Polymer Microstructure,* VCH Publishers, New York, 1989.
17. N. Probst, Ph.D. Thesis, Hamburg, 1996.
18. C. Wutz, *Polymer,* **39(1),** 1 (1998).
19. C. A. Fyfe, J. R. Lyerla, W. Volksen, and C. S. Yannoni, *Macromolecules,* **12,** 757 (1979).
20. J. Schaefer, E. O. Stejskal, and R. Buchdahl, *Macromolecules,* **10,** 384 (1977).
21. C. Wutz, D. Schleyer, and H. R. Kricheldorf, *J. Polym. Sci.: B: Polym. Phys.,* submitted (1997).
22. L. Abis and E. Merlo, *J. Polym. Sci.: Polym. Phys. Ed.,* **B33,** 691 (1995).
23. S. Dreher, Ph.D. Thesis, *Universität Hamburg,* Shaker Verlag, Aachen, 1996.
24. L. Müller, A. Kumar, T. Baumann, and R. R. Ernst, *Phys. Rev. Lett.,* **32,** 1402 (1974).
25. D. Y. Yoon and S. Bruckner, *Macromolecules,* **18,** 651 (1985).
26. N. Probst, C. Wutz, and H. R. Kricheldorf, *Macromolecules,* submitted (1997).
27. C. Wutz, *Mol. Cryst. Liq. Cryst.,* **307,** 175–188 (1997).
28. C. Wutz, T. Maevis, D. Gieseler, and N. Stribeck, *Orientation of the Mesogens in Smectic Poly(ester imide) Fibers,* to be published.
29. C. Wutz et al., to be published.
30. K. Schmidt-Rohr, J. Clauss, and H. W. Spiess, *Macromolecules,* **25,** 3273 (1992).
31. C. Schmidt-Rohr, and H. W. Spiess, Eds., *Multidimensional Solid-State NMR and Polymers,* Academic Press, San Diego, 1994, Chap. 6, p. 213.
32. J. Clauss, K. Schmidt-Rohr, A. Adam, C. Boeffel, and H. W. Spiess, *Macromolecules,* **25,** 5208 (1995).
33. R. K. Harris, Ed., *Nuclear Magnetic Resonance Spectroscopy,* Pitman, London, 1983, p. 107.